

THE INCIDENCE OF ACTIVE GALACTIC NUCLEI IN PURE DISK GALAXIES: THE *SPITZER* VIEW

S. SATYAPAL¹, T. BÖKER², W. MCALPINE¹, M. GLIOZZI¹, N. P. ABEL³, & T. HECKMAN⁴

Draft version October 31, 2021

ABSTRACT

Using the *Spitzer* telescope, we have conducted a high-resolution spectroscopic study of 18 bulgeless (Hubble type of Sd or Sdm) galaxies that show no definitive signatures of nuclear activity in their optical spectra. This is the first systematic mid-infrared search for weak or hidden active galactic nuclei (AGNs) in a statistically significant sample of bulgeless (Sd/Sdm) disk galaxies. Based on the detection of the high-ionization [NeV] 14.3 μm line, we report the discovery of an AGN in one out of the 18 galaxies in the sample. This galaxy, NGC 4178, is a nearby edge-on Sd galaxy, which likely hosts a prominent nuclear star cluster (NSC). The bolometric luminosity of the AGN inferred from the [NeV] line luminosity is $\sim 8 \times 10^{41}$ ergs s⁻¹. This is almost two orders of magnitude greater than the luminosity of the AGN in NGC 4395, the best studied AGN in a bulgeless disk galaxy. Assuming that the AGN in NGC 4178 is radiating below the Eddington limit, the lower mass limit for the black hole is $\sim 6 \times 10^3 M_{\odot}$. The fact that none of the other galaxies in the sample shows any evidence for an AGN demonstrates that while the AGN detection rate based on mid-infrared diagnostics is high (30-40%) in optically quiescent galaxies with pseudobulges or weak classical bulges (Hubble type Sbc and Sc), it drops drastically in Sd/Sdm galaxies. Our observations therefore confirm that AGNs in completely bulgeless disk galaxies are *not* hidden in the optical but truly are rare. Of the three Sd galaxies with AGNs known so far, all have prominent NSCs, suggesting that in the absence of a well-defined bulge, the galaxy must possess a NSC in order to host an AGN. On the other hand, while the presence of a NSC appears to be a requirement for hosting an AGN in bulgeless galaxies, neither the properties of the NSC nor those of the host galaxy appear exceptional in late-type AGN host galaxies. The recipe for forming and growing a central black hole in a bulgeless galaxy therefore remains unknown.

Subject headings: Galaxies: Active— Galaxies: black hole physics – dark matter – galaxies: spiral: Galaxies — Infrared: Galaxies

1. INTRODUCTION

We now know that supermassive black holes lurk in the centers of most bulge-dominated galaxies in the local Universe and that their black hole masses, M_{BH} , and the stellar velocity dispersions, σ , of their host galaxies are strongly correlated (Gebhardt et al. 2000, Ferrarese & Merritt 2000). This discovery has launched numerous speculations that the formation and evolution of galaxies and supermassive black holes are fundamentally linked, and that perhaps the presence of a bulge is a necessary ingredient for a black hole to form and grow. Indeed, M33, the most nearby example of a truly bulgeless disk galaxy shows no evidence of a supermassive black hole, and the upper limit on the black hole mass determined by stellar dynamical studies is significantly below that predicted by the $M_{\text{BH}}-\sigma$ relation established in early-type galaxies (e.g., Gebhardt et al. 2001). In contrast, the disk galaxy NGC 4395 shows no evidence for a bulge and yet does contain an active nucleus (e.g., Filippenko & Ho 2003). However, this galaxy has remained until recently the only case of a truly bulgeless disk galaxy with an accreting black hole, leaving open the possibility that it is an anomaly. Indeed, prior to the launch of *Spitzer*, the

vast majority of known accreting black holes - i.e., active galactic nuclei (AGN) - in the local Universe were found in galaxies with prominent bulges (e.g. Heckman 1980; Ho, Filippenko, & Sargent 1997; Kauffmann et al. 2003).

However, these studies were based on spectroscopic observations at optical wavelengths, which can be severely limited in the study of bulgeless galaxies, where a putative AGN is likely to be both energetically weak and deeply embedded in the center of a dusty late-type spiral. In such systems, the traditional optical emission lines used to identify AGN can be dominated by emission from star formation regions, in addition to being significantly attenuated by dust in the host galaxy. As a result, it is by no means clear what fraction of late-type galaxies host AGN. Therefore, some key fundamental questions on the connection between black holes and galaxy formation and evolution have yet to be answered, such as: What fraction of late-type galaxies host AGNs? Do black holes form and grow in galaxies without a bulge? How are the incidence and properties of the black hole related to the host galaxy in cases where there is no bulge?

Motivated by these questions, and by the possibility that optical studies may fail at finding AGNs in the latest Hubble types, we have previously conducted an exhaustive archival mid-infrared (MIR) spectroscopic investigation of 34 late-type (Sbc or later) galaxies observed by *Spitzer* to search for AGNs (Satyapal et al. 2007; Satyapal et al. 2008 - henceforth S07; S08, respectively). Remarkably, these observations revealed the presence of the high ionization [NeV] 14 μm and/or 24 μm lines - which are not generally produced in ionized gas surrounding hot

¹ George Mason University, Department of Physics & Astronomy, MS 3F3, 4400 University Drive, Fairfax, VA 22030; satyapal@physics.gmu.edu

² ESA/ESTEC, Keplerlaan1, 2200AG Noordwijk, Netherlands

³ Department of Physics, University of Cincinnati, Cincinnati, OH 45221

⁴ Center for Astrophysical Sciences, Department of Physics and Astronomy, The Johns Hopkins University, Baltimore, MD 21218

stars - in a significant number of galaxies that have no clear signatures of an AGN in their optical spectra. Using detailed photoionization models with both an input AGN and an extreme EUV-bright radiation field from a young starburst, we demonstrated that the MIR spectrum of these galaxies cannot be replicated unless an AGN contribution, in some cases as weak as 10% of the total galaxy luminosity, is included (S08, Abel & Satyapal 2007). *This implies that the AGN detection rate in late-type galaxies is possibly more than 4 times larger than what optical spectroscopic studies alone indicate.* We have obtained follow-up X-ray observations of a subset of these galaxies, which in all cases confirm the presence of an AGN (Gliozzi et al. 2009; Satyapal et al. 2009). A more recent *Spitzer* study has also uncovered a significant population of AGNs in optically quiescent galaxies of earlier Hubble type (Goulding & Alexander 2009), demonstrating the power of mid-infrared spectroscopy in AGN searches. Other recent multiwavelength studies have also shown that AGNs are significantly more common in late-type galaxies than once thought (e.g., Greene, Ho, & Barth 2009; Shields et al. 2008; Ghosh et al. 2008; Barth et al. 2009; Dewangan et al. 2008; Desroches & Ho 2009). It is therefore clear that classical bulges are *not* required for black holes to form and grow.

While it is evident that AGNs do reside in a significant number of late-type galaxies, most of the galaxy hosts appear to have a pseudobulge component, i.e. a central light excess characterized by an exponential surface brightness profile. These pseudobulges are thought to form via secular processes, in contrast to the violent merger-driven formation history of classical bulges (Kormendy & Kennicutt 2004). Amongst our previous archival *Spitzer* sample, there were only 4 very late-type spirals (Hubble type Sd/Sdm) without any obvious sign of a pseudo-bulge. We discovered prominent [NeV] emission from only one of these sources - the nearby Sd galaxy NGC 3621 (S07). Follow-up X-ray (Gliozzi et al. 2009) and high spatial resolution optical (Barth et al. 2009) observations confirm the presence of an AGN in this source. NGC 3621 is similar to NGC 4395 in that both galaxies are essentially bulgeless and contain a massive nuclear star cluster (Barth et al. 2009). However, with only two examples and only a total of 4 truly bulgeless disk galaxies observed, it is not possible to determine robustly the fraction of AGNs in pure disk galaxies and to understand how the incidence and properties of black holes relate to the host galaxy in the absence of a bulge.

In this paper, we present results from a recent *Spitzer* MIR spectroscopic investigation of 18 optically quiescent, truly bulgeless disk galaxies in order to search for previously undetected low luminosity and/or embedded AGN. This is the first systematic MIR search for weak or hidden AGN in a statistically significant sample of "pure" disk galaxies. The primary goal of this paper is to refine the incidence of AGNs in this type of galaxy. As our previous *Spitzer* work has demonstrated, optical studies miss a significant fraction of AGNs in late-type galaxies, leaving open the possibility that there are a significant number of active black holes in the centers of completely bulgeless galaxies that are as yet undiscovered.

This paper is structured as follows. In Section 2, we summarize the properties of the *Spitzer* sample presented in this paper. In Section 3, we summarize the observa-

tional details and data analysis procedure, followed by a description of our results in Section 4. In Section 5, we discuss the origin of the [NeV] emission and the evidence for an AGN in our sample, followed by a discussion of the AGN detection rate in pure disk galaxies in Section 6. In Section 7, we investigate the demographics of late-type galaxies with AGNs, followed by an exploration in Section 8 of the host characteristics of the few AGNs that reside in definitively bulgeless galaxies. A summary of our major conclusions is given in Section 9.

2. THE SAMPLE

Our goals in selecting a sample were to 1) obtain a statistically significant sample of pure (i.e. bulgeless) disk galaxies to provide meaningful estimates of the fraction that host AGNs, 2) select close-by objects to enable detailed follow-up of potential AGN discoveries, 3) select isolated disk galaxies to avoid the effects of interactions on triggering black hole formation and growth and to test whether black holes routinely form through purely secular processes, and 4) select well-studied sources with extensive optical spectroscopic and multiwavelength data available in the literature. Our target sources were selected from the Palomar survey of nearby bright galaxies (Ho et al. 1997; henceforth H97). Of the 486 galaxies in the Palomar survey, a little more than two-dozen are of Hubble type of Sd/Sdm. Excluding galaxies with irregular morphologies or other signs of interactions, and excluding the well-studied Seyfert NGC 4395, our final sample contained 18 galaxies.

Table 1 summarizes the basic properties of the galaxies in our sample. All targets are nearby, ranging in distance from 2.4 to 21.6 Mpc, with an average distance of ~ 11 Mpc. The aperture of the optical measurements from H97 was $2'' \times 4''$. The extinction-corrected absolute B-band magnitude ranges from ~ -17 to -20 . We estimate and list in Table 1 galaxy stellar masses using the extinction-corrected B-V color and absolute B magnitude using the mass-to-light ratios from Bell et al. (2003). The inferred galaxy masses for our sample range from $\sim 8 \times 10^8 M_{\odot}$ to $\sim 1.6 \times 10^{10} M_{\odot}$. The distribution of derived galaxy masses of the sample is shown in Figure 1. We also list in Table 1 the nuclear star formation rate (SFR), estimated using the extinction-corrected H α luminosity from H97, assuming all of the H α luminosity arises from star forming regions, and using the prescription given in Kennicutt (1998). The SFR ranges from $\sim 6 \times 10^{-5} M_{\odot}/\text{yr}$ to $\sim 2 \times 10^{-3} M_{\odot}/\text{yr}$. The (inclination-corrected) line width of the HI profile, also from H97, ranges from 21 to 314 km/s, suggesting that the sample spans a large range of dark matter mass. To determine whether the presence or properties of potential AGNs are related in any way to gas mass, we list in Table 1 the HI mass, estimated from the HI fluxes compiled in H97.

The majority of galaxies in our sample are classified in H97 as "HII" stellar-powered galaxies; only two are "T2" transition galaxies. T2 galaxies have optical line ratios intermediate between HII galaxies and low-ionization nuclear emission-line regions (LINERs) and have no broad permitted lines (e.g. H α) in their optical spectrum. There is therefore no firm optical spectroscopic evidence for AGNs in any of the galaxies in our sample. This is illustrated in Figure 2 which shows the standard optical line ratio diagnostic diagrams (Veilleux & Oster-

Table 1: Properties of the Sample

| Galaxy Name | Distance (Mpc) | [OIII]/H β | [OI]/H α | [NII]/H α | [SII]/H α | Optical Class | M $_{BT}^0$ | M $_{Gal}$ (M $_{\odot}$) | M $_{HI}$ (M $_{\odot}$) | ΔV_{rot} (km/s) | NC | SFR (10 $^{-3}$ M $_{\odot}$ /yr) |
|-------------|----------------|------------------|-----------------|------------------|------------------|---------------|-------------|----------------------------|---------------------------|-------------------------|----------|-----------------------------------|
| IC 2574 | 3.4 | 0.23 | 0.025 | 0.07 | 0.25 | H | -17.33 | 8.91 | 9.05 | 131 | Unlikely | 0.16 |
| NGC 2500 | 10.1 | 2.42 | 0.068 | 0.33 | 0.45 | H | -18.03 | 9.40 | 8.91 | 228 | Yes | 0.14 |
| NGC 2537 | 9 | 1.83 | 0.008 | 0.15 | 0.18 | H | -17.75 | 9.29 | 8.59 | 205 | ... | 27.81 |
| NGC 3027 | 19.5 | 1.16 | 0.037 | 0.19 | 0.53 | H | -19.77 | 10.10 | 9.93 | 247 | ... | 3.99 |
| NGC 3432 | 7.8 | 1.71 | 0.012 | 0.14 | 0.22 | H | -18.43 | 9.56 | 9.26 | 260 | Maybe | 5.47 |
| NGC 3495 | 12.8 | 0.38 | 0.05 | 0.42 | 0.43 | H | -19.8 | 10.11 | 9.17 | 314 | ... | 0.67 |
| NGC 4145 | 20.7 | 1.09 | 0.13 | 0.61 | 0.8 | T2 | -20.04 | 10.21 | 9.82 | 21 | ... | 1.68 |
| NGC 4178 | 16.8 | 0.35 | 0.022 | 0.32 | 0.5 | H | -19.78 | 10.10 | 9.66 | 299 | Yes | 5.16 |
| NGC 4242 | 7.5 | 1 | 0.27 | 0.27 | 0.91 | H | -18.08 | 9.42 | 8.78 | 206 | Yes | 0.06 |
| NGC 4618 | 7.3 | 1.82 | 0.012 | 0.16 | 0.23 | H | -18.19 | 9.47 | 9.04 | 220 | Yes | 4.75 |
| NGC 4656 | 7.2 | 4.02 | 0.022 | 0.05 | 0.18 | H | -19.19 | 9.87 | 9.62 | 179 | Unlikely | 2.05 |
| NGC 4713 | 17.9 | 1.01 | 0.087 | 0.44 | 0.67 | T2 | -19.41 | 9.96 | 9.64 | 242 | Yes | < 3.14 |
| NGC 5147 | 21.6 | 0.44 | 0.035 | 0.37 | 0.52 | H | -19.38 | 9.94 | 9.30 | 259 | ... | 4.14 |
| NGC 5204 | 4.8 | 0.96 | 0.099 | 0.18 | 0.56 | H | -16.93 | 8.96 | 8.76 | 154 | Maybe | < 0.38 |
| NGC 5585 | 7 | 1.7 | 0.017 | 0.15 | 0.32 | H | -18.18 | 9.46 | 9.19 | 200 | Yes | 2.63 |
| NGC 6689 | 12.2 | 1.87 | 0.067 | 0.4 | 0.62 | H | -18.48 | 9.58 | 9.13 | 220 | Unlikely | 0.79 |
| NGC 784 | 4.7 | 4.9 | 0.006 | 0.03 | 0.09 | H | -17.2 | 9.07 | 8.54 | 116 | Unlikely | < 0.96 |
| NGC 959 | 10.1 | 1.16 | 0.032 | 0.34 | 0.37 | H | -17.66 | 9.26 | 8.45 | 196 | Yes | 2.09 |

Columns Explanation: Col(1): Common Source Names; Col(2): Distance to the source in units of Mpc are all taken directly from H97 where distances are adopted from Tully & Shaya (1984); Col(3): [OIII] to H β ratio taken from H97; Col(4): [OI] to H α ratio taken from H97; Col (5): [NII] to H α ratio taken from H97; Col(6): [SII] to H α ratio taken from H97; Col(7): Optical classification of the source; “H” signifies HII region ratios, “T” represents transitional spectra between LINERs and HII regions, and “2” indicates that broad permitted lines were not found in the optical spectrum. Col(8): Total absolute B magnitude corrected for extinction, adopted from H97; Col(9): Galactic Mass obtained from B-V color and B-magnitude from H97 using mass-to-light ratios from Bell et al. (2003); Col(10): HI mass taken from H97; Col(11): Inclination-corrected HI rotational amplitude taken directly from Table 10, col(7) in H97; Col(12) Presence of Nuclear Cluster based on archival *HST* observations. Col (13) Nuclear star formation rate estimated using the extinction-corrected H α luminosity from H97, assuming all of the H α luminosity arises from star forming regions, and using the prescription given in Kennicutt (1998)

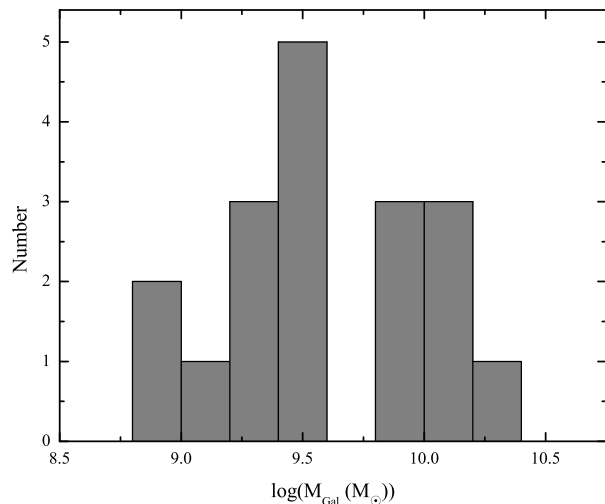


FIG. 1.— The distribution of galaxy masses for the sample. Galaxy masses were estimated using the extinction-corrected B-V color and B-band magnitude taken directly from H97 using the M/L ratios from Bell et al. (2003)

brock 1987) widely used to classify AGNs for the entire H97 sample. Our Spitzer sample is highlighted, together with the theoretical starburst limit line from Kewley et al. 2001, i.e. the maximum line ratios allowed by starburst photoionization models using the hardest possible radiation field. Note that the majority of galaxies in our sample have optical line ratios well to the left of this line, indicating that the optical line ratios do not require the presence of *any* AGN contribution.

As can be seen from the DSS images in Figure 3, the morphologies of the sample galaxies are varied, with some objects having prominent disks and clear photocenters, and others displaying a more diffuse structure with no

obvious photocenter. Archival *HST* images are available for 14 out of the 18 galaxies in the sample, taken mostly with the *Advanced Camera for Surveys* (ACS). We inspected these images for the presence of a well-defined nuclear star cluster (NSC). An unambiguous detection of such a source was possible in 7 of the 14 sample galaxies. These galaxies are identified in Table 1. We also performed elliptical isophote fitting to check for a notable bulge component in the one-dimensional surface brightness profiles, and confirmed that all of the sample galaxies are pure disk galaxies.

3. OBSERVATIONS AND DATA REDUCTION

Data for all but one of the galaxies in our sample were obtained from the *Spitzer* Cycle 5 GO program ID 50339 (PI: Satyapal). These observations were all executed between 2008 June and 2008 November. One of the galaxies in our sample (NGC 4618) was previously observed with the IRS in 2005 December (PID 20140). We used the archival data for this galaxy. All observations were carried out in staring mode using both the short-wavelength (SH, 4.7” \times 11.3”, λ = 9.9-19.6 μ m) and long-wavelength (LH, 11.1” \times 22.3”, λ = 18.7-37.2 μ m) high-resolution modules of the Infrared Spectrograph (IRS; Houck et al. 2004) which have a spectral resolution of R \sim 600. Exposure times were chosen to provide a signal-to-noise ratio of at least 5 for the [NeV] 14.3 μ m line, assuming the lowest [NeV] luminosity detected to date in any galaxy (S08). Each observation was followed by a background sky observations located 2’ from the source in order to enable background-subtraction.

All on-source observations were centered on the galaxy nuclei, i.e. the photocenter coordinates from H97, which agree well with the 2MASS coordinates. Figure 3 overlays the SH and LH slit apertures onto the DSS images for all our targets, demonstrating that the nucleus of the galaxy always falls well within the slit. The slit size for the median distance of 10 Mpc corresponds to a projected extraction aperture of 0.2 kpc \times 0.5 kpc and 0.5

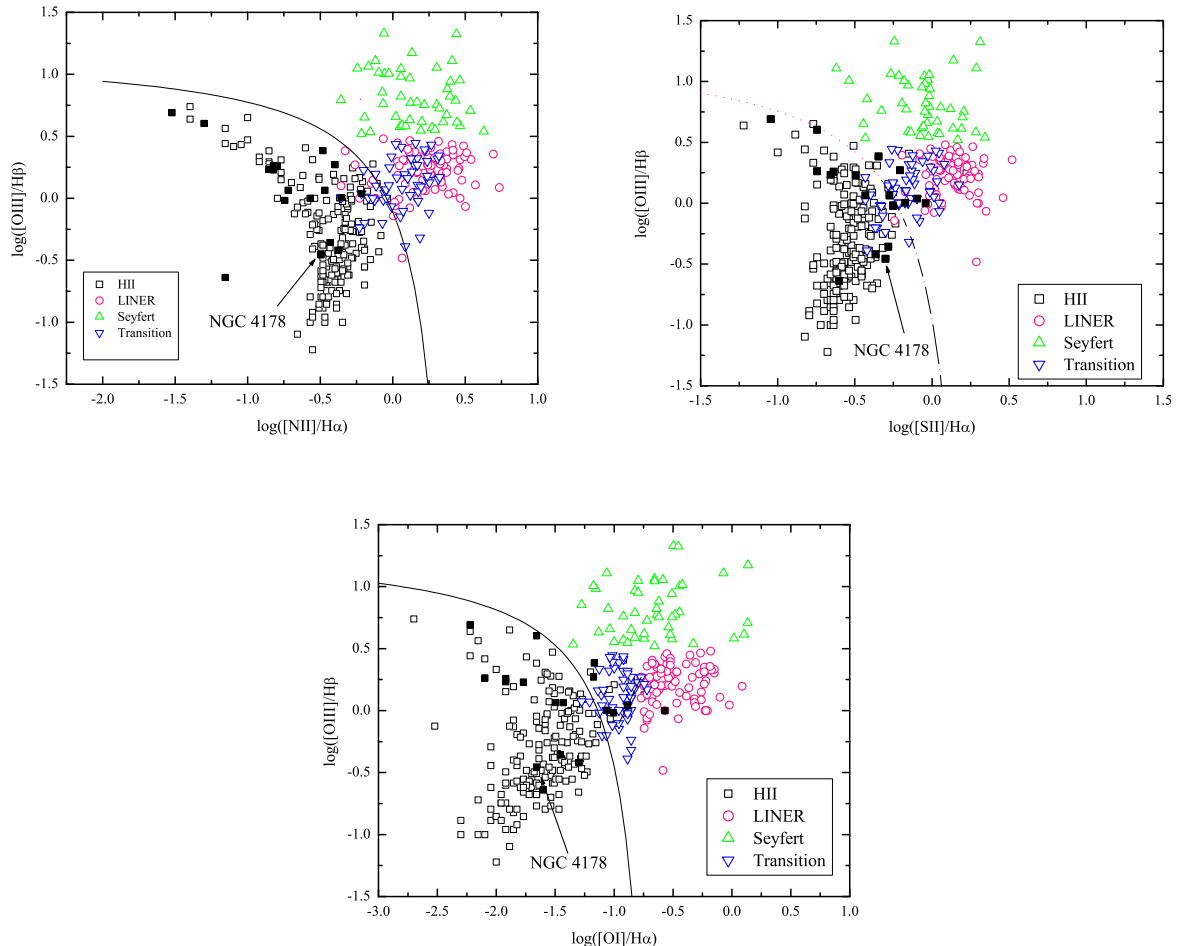


FIG. 2.— Standard optical line ratio diagnostic diagrams (Veilleux & Osterbrock 1987) for the entire H97 sample with our current *Spitzer* sample highlighted by filled symbols. The solid line indicates the theoretical starburst limit from Kewley et al. 2001. This limit marks the maximum line ratios possible from starburst-only photoionization models. NGC 4178, the only galaxy in our sample with a [NeV] detection, is labeled in the figure. The optical line ratios for this galaxy are well to the left of the starburst limit, indicating that the optical line ratios are consistent with ionization by star formation only.

kpc \times 1.1 kpc for the SH and LH modules, respectively. The projected slit sizes, as well as a number of other observational details, are listed in Table 2.

We note that the SH and LH staring observations are dithered, i.e. the integration is split into two slit positions overlapping by one third of a slit. Unless the emission originates from a compact source that falls entirely within the slit for both pointings, the two spectra cannot be averaged. The procedure for flux extraction for staring observations was the following: 1) If the fluxes measured from the two slits differed by no more than the calibration error of the instrument, then the fluxes were averaged; otherwise, the slit with the highest measured line flux was chosen. 2) If an emission line was detected in one slit, but not in the other, then the detection was selected. The overall calibration uncertainty for the fluxes we report in this paper is 15%.

The raw data were preprocessed by the IRS pipeline (version 17.2) at the *Spitzer* Science Center (SSC) prior to download. Preprocessing includes ramp fitting, dark-

sky subtraction, droop correction, linearity correction, flat-fielding, and flux calibration². The *Spitzer* spectra were further processed using the SMART v. 6.3.0 analysis package (Higdon et al. 2004) and the corresponding version of the calibration files (v.1.5.0), which were used to obtain final line fluxes. Each spectra was individually inspected and any bad pixels remaining after pipeline processing were removed. The fine-structure line fluxes presented in this work were obtained from Gaussian fits to the spectral line and linear fits to the baseline continuum.

Many of the galaxies in our sample display prominent PAH features and molecular hydrogen emission lines. In this work, we limit the discussion to the fine-structure emission lines relevant for identification of potential AGN. We defer discussion of all other spectral diagnostics and the star-formation properties of bulge-

² See *Spitzer* Observers Manual, Chapter 7, <http://ssc.spitzer.caltech.edu/documents/som/som8.0.irs.pdf>

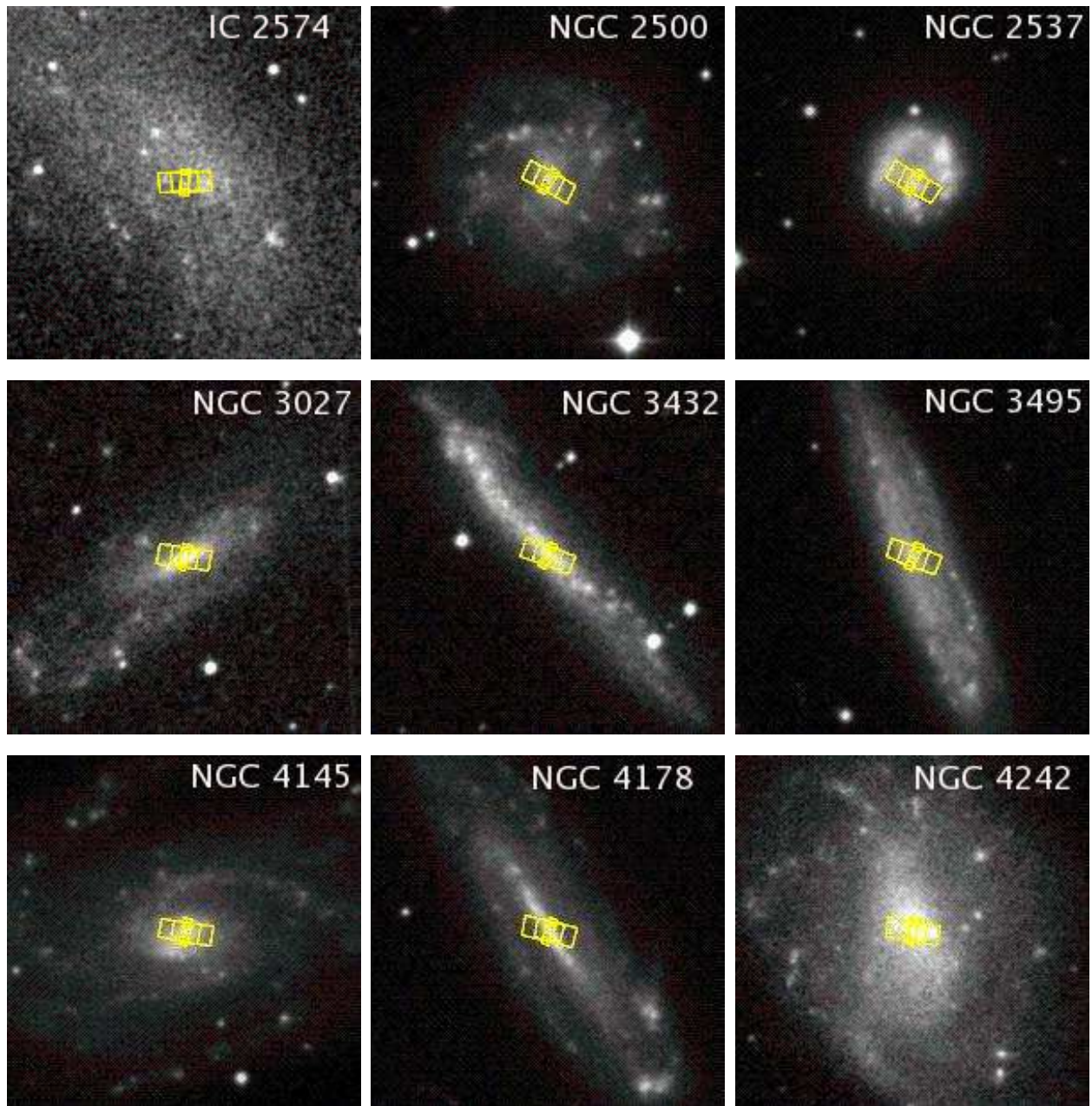


FIG. 3.— DSS images of the galaxies in the sample with IRS SH and LH slits overlaid. The field of view of the images is $200'' \times 200''$.

less galaxies to a future paper.

4. RESULTS

4.1. *Fine-Structure Line Fluxes*

In Table 3 we list the line fluxes, statistical errors and 3σ upper limits for the strongest MIR fine-structure lines. The apertures from which these fluxes were extracted are listed in Table 2. In all cases, detections were defined when the line flux was at least 3σ . The strongest emission features in the spectra were the [NeII] $12.8 \mu\text{m}$, [NeIII] $15.5 \mu\text{m}$, [SIII] $18.7 \mu\text{m}$, [SIII] $33.5 \mu\text{m}$, and [SiIII] $34.8 \mu\text{m}$ lines, detected in $\sim 60\%$ - 80% of the galaxies in the sample. The [FeII] $26 \mu\text{m}$, [NeV] $24 \mu\text{m}$, and [OIV] $25.9 \mu\text{m}$ emission lines were not detected in any galaxy in

the sample. We note that the spectral resolution of the SH and LH modules of the IRS is insufficient to resolve the velocity structure for most of the lines. We detected the [NeV] $14.3 \mu\text{m}$ line in only 1 out of the 18 galaxies, providing strong evidence for the presence of an AGN in this one galaxy. We discuss the IR spectral line fluxes and flux ratios for this galaxy, NGC 4178, separately in Section 5 below.

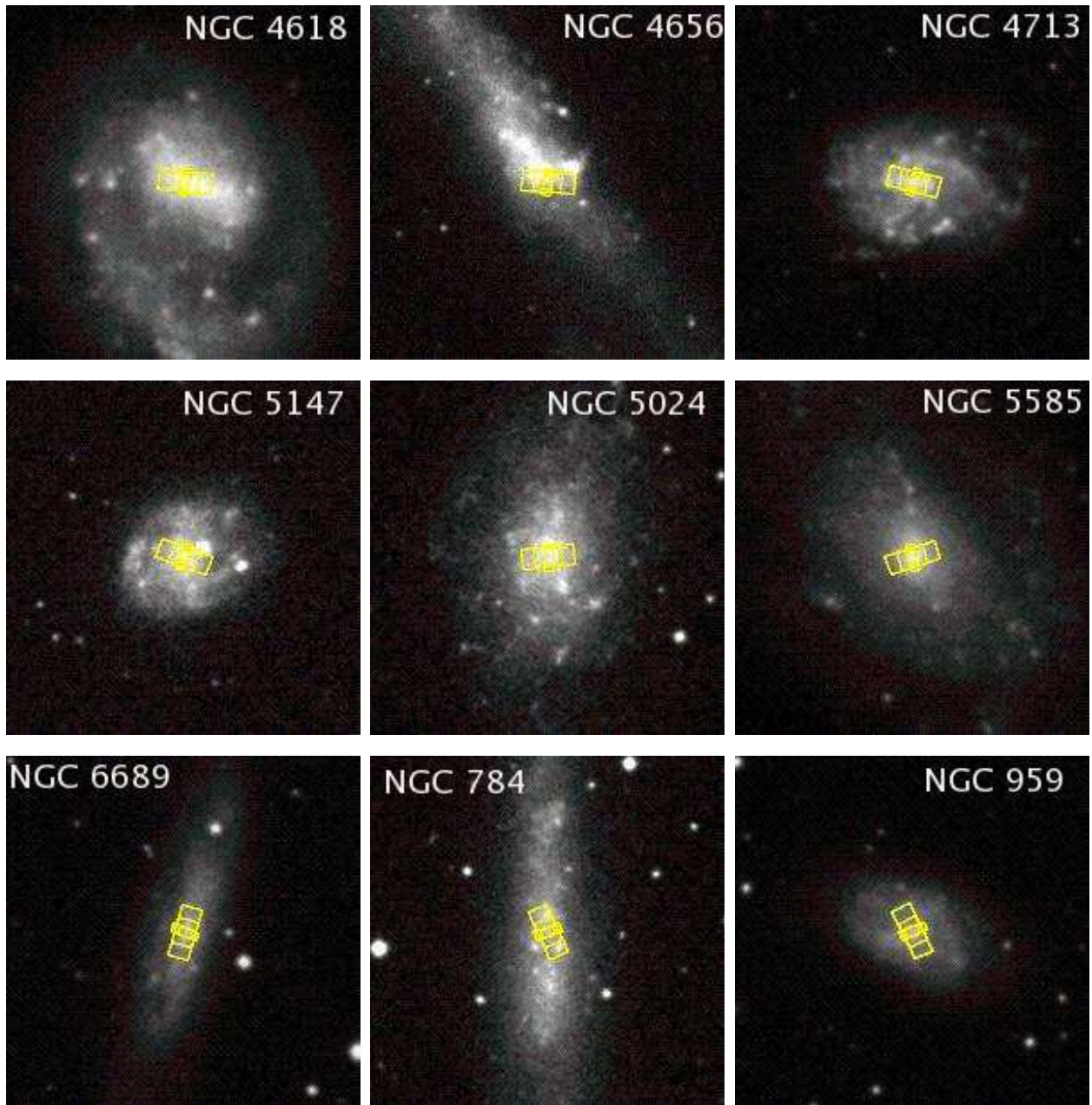
FIG 3.-*Continued*

Table 2: Observational Details

| Galaxy Name | Exposure Time SH (seconds) | Exposure Time LH (seconds) | Position (J2000) | | Extraction Aperture Size SH (pc) | Extraction Aperture Size LH (pc) |
|-------------|----------------------------|----------------------------|------------------|--------------|----------------------------------|----------------------------------|
| | | | RA | Dec | | |
| IC2574 | 6×3 | 6×3 | 10 28 23.50 | +68 24 44.00 | 77×186 | 183×368 |
| NGC2500 | 30×3 | 14×3 | 08 01 53.21 | +50 44 13.60 | 230×553 | 544×1092 |
| NGC2537 | 30×2 | 14×3 | 08 13 14.60 | +45 59 23.30 | 205×493 | 484×973 |
| NGC3027 | 120×3 | 240×3 | 09 55 40.60 | +72 12 12.80 | 444×1068 | 1049×2108 |
| NGC3432 | 30×2 | 14×2 | 10 52 31.13 | +36 37 07.60 | 178×427 | 420×843 |
| NGC3495 | 30×4 | 60×3 | 11 01 16.23 | +03 37 40.50 | 292×701 | 689×1384 |
| NGC4145 | 120×4 | 240×4 | 12 10 01.52 | +39 53 01.90 | 472×1134 | 1114×2238 |
| NGC4178 | 120 ×2 | 240×2 | 12 12 46.40 | +10 51 57.50 | 383×920 | 904×1816 |
| NGC4242 | 30×2 | 14×2 | 12 17 30.18 | +45 37 09.50 | 171×411 | 404×811 |
| NGC4618 | 30×2 | 60×2 | 12 11 32.85 | +41 09 02.80 | 166×400 | 393×789 |
| NGC4656 | 30×2 | 14×2 | 12 43 57.73 | +32 10 05.30 | 164×394 | 387×778 |
| NGC4713 | 120×2 | 240×2 | 12 49 57.87 | +05 18 41.10 | 408×981 | 963×1935 |
| NGC5147 | 120×4 | 240×5 | 13 26 19.71 | +02 06 02.60 | 492×1183 | 1162×2335 |
| NGC5204 | 6×3 | 6×3 | 13 29 36.51 | +58 25 07.40 | 109×263 | 258×519 |
| NGC5585 | 30×2 | 14×2 | 14 19 48.20 | +56 43 44.60 | 160×383 | 377×757 |
| NGC6689 | 30×3 | 60×2 | 18 34 50.25 | +70 31 26.10 | 278×668 | 657×1319 |
| NGC784 | 6×3 | 6×3 | 02 01 16.93 | +28 50 14.10 | 107×257 | 253×508 |
| NGC959 | 30×2 | 14×3 | 02 32 23.94 | +35 29 40.70 | 230×553 | 544×1092 |

Columns Explanation: Col(1): Common Source Names; Col(2) & (3): On-source exposure time per pointing in seconds given for the SH and LH modules, respectively; Col(4) & (5): Coordinates used for each observations; Col(6) & (7): Extraction apertures for the SH and LH modules, which correspond to the full aperture of the slit. Values given are in parsecs, using galaxy distances listed in Table 1.

Table 3: Fine-Structure Line Fluxes

| Name | [SIV] 10.51 μ m | [NeII] 12.81 μ m | [NeV] 14.32 μ m | [NeIII] 15.56 μ m | [SIII] 18.71 μ m | [NeV] 24.32 μ m | [OIV] 25.89 μ m | [FeII] 25.99 μ m | [SIII] 33.48 μ m | [SiII] 34.82 μ m |
|---------|---------------------|----------------------|---------------------|-----------------------|----------------------|---------------------|---------------------|----------------------|----------------------|----------------------|
| IC2574 | <19.95 | <10.25 | <19.31 | <13.18 | <30.29 | <22.96 | <24.47 | <24.56 | <89.63 | <119.89 |
| NGC2500 | <6.46 | <3.87 | <5 | <3.69 | <5.34 | <9.69 | <10.32 | <10.36 | 90 \pm 19 | <27.51 |
| NGC2537 | <5.88 | 9.6 \pm 2.76 | <3.4 | <3.95 | <4.15 | <8.16 | <8.69 | <8.72 | 43 \pm 13 | <43.89 |
| NGC3027 | 7.6 \pm 1.02 | 6.13 \pm 0.62 | <0.48 | 3.1 \pm 0.6 | 4.81 \pm 0.55 | <2.62 | <2.8 | <2.81 | 21.5 \pm 2.88 | 21.2 \pm 2.46 |
| NGC3432 | 8.1 \pm 1.75 | 28.1 \pm 2.5 | <3.71 | 30.2 \pm 3.4 | 28.9 \pm 2.16 | <7.75 | <8.25 | <8.29 | 198.5 \pm 15.16 | 122.5 \pm 8.59 |
| NGC3495 | <2.95 | 13.3 \pm 1.3 | <1.88 | 12.2 \pm 1.6 | 14 \pm 3.8 | <5.45 | <5.81 | <5.83 | 32.9 \pm 9 | 39.7 \pm 7.5 |
| NGC4145 | 5.13 \pm 1.42 | 7.55 \pm 0.87 | <0.64 | 2.77 \pm 0.36 | 3.65 \pm 0.55 | <1.89 | <2.02 | <2.03 | 17 \pm 7.19 | 22.8 \pm 0.65 |
| NGC4178 | <1.23 | 20.9 \pm 1.95 | 2.43 \pm 0.39 | 5.95 \pm 0.45 | 12.82 \pm 0.89 | <2.79 | <2.11 | <2.14 | 80.7 \pm 4.6 | 83.7 \pm 2.53 |
| NGC4242 | <2.83 | <3.78 | <3.47 | <4.58 | <5.26 | <9.44 | <10.05 | <10.09 | <26.44 | <31.15 |
| NGC4496 | <5.49 | <6.53 | <3.58 | <4.5 | <6.6 | <5.44 | <5.8 | <5.82 | <9.19 | <15.38 |
| NGC4618 | <8.24 | 36.59 \pm 6.62 | <4.78 | 24.91 \pm 3.88 | 24.51 \pm 1.94 | <8.84 | <9.6 | <9.64 | 63.23 \pm 6.82 | 49.41 \pm 6.25 |
| NGC4656 | 47.3 \pm 5.25 | 40 \pm 1.7 | <3.5 | 41.8 \pm 2.65 | 23.8 \pm 3.7 | <6.82 | <7.26 | <7.29 | 128 \pm 15.49 | 97.8 \pm 14 |
| NGC4713 | <1.97 | 15.85 \pm 1.58 | <1.85 | 5.47 \pm 0.92 | 7.96 \pm 1.07 | <2.21 | <2.36 | <2.37 | 92.2 \pm 4.18 | 94.9 \pm 2.63 |
| NGC5147 | <1.46 | 9.06 \pm 1.09 | <1 | 3.6 \pm 0.42 | 4.96 \pm 0.7 | <2.3 | <2.45 | <2.46 | 28.8 \pm 3.47 | 32.8 \pm 2.13 |
| NGC5204 | <16.99 | <8.06 | <9.01 | <11.16 | 51.4 \pm 7.25 | <10.57 | <11.26 | <11.31 | 165 \pm 54.3 | <78.34 |
| NGC5585 | <2.52 | 11.6 \pm 2.9 | <2.04 | 11.7 \pm 2.15 | 17.1 \pm 2.74 | <7.48 | <7.97 | <8 | 53.5 \pm 14 | 67.8 \pm 16.3 |
| NGC6689 | <3.68 | <3.32 | <3.14 | <2.68 | <4.96 | <5.94 | <6.33 | <6.36 | 36.35 \pm 9.59 | 32 \pm 3.8 |
| NGC784 | <20.97 | <10.25 | <17.93 | 45 \pm 18.3 | <26.21 | <16.4 | <17.48 | <17.54 | <34.07 | <82.68 |
| NGC959 | <5.15 | <3.42 | <3.69 | 9.25 \pm 1.9 | <5.92 | <7.7 | <8.21 | <8.24 | 60.3 \pm 12 | 47.7 \pm 14.2 |

Columns Explanation: Col(1): Common Source Names; Col(2)-Col(11)): Fluxes are in units of 10^{-22} W cm $^{-2}$. 3 σ upper limits are reported for nondetections.

4.2. Incidence of AGN

The absence of [NeV] (ionization potential 97 eV) emission in our sample strongly suggests that with the exception of NGC 4178, none of the galaxies in our sample harbor AGNs. In Table 4, we list the [NeV] $14.3 \mu\text{m}$ luminosities corresponding to the 3σ upper limits on the fluxes for all galaxies in the sample with the exception of NGC 4178. The luminosities were obtained using the galaxy distances listed in Table 1. The upper limits to the line luminosity are well below $10^{38} \text{ ergs s}^{-1}$. Using the compilations of MIR line fluxes of standard AGN from Sturm et al. (2002), Haas et al. (2005), Weedman et al. (2005), Ogle et al. (2006), Cleary et al. (2007), Armus et al. (2007), Gorjian et al. (2007), Deo et al. (2007), Tommasin et al. (2008), and Dale et al. (2009)², there are 82 standard AGNs (optically classified as type 1 or type 2 AGN) with measured [NeV] $14\mu\text{m}$ line fluxes. The [NeV] $14 \mu\text{m}$ line luminosities for these AGNs range from $\sim 2 \times 10^{38} \text{ ergs s}^{-1}$ to $\sim 8 \times 10^{42} \text{ ergs s}^{-1}$ with a median value of $\sim 5 \times 10^{40} \text{ ergs s}^{-1}$, more than two orders of magnitude above the [NeV] limiting sensitivities listed in Table 4. The [NeV] luminosity of NGC 3621, our one and only previously discovered Sd galaxy with a weak AGN is $\sim 5 \times 10^{37} \text{ ergs s}^{-1}$ (S07), consistent with or above the limiting sensitivities of $\sim 90\%$ of our sample. Our non-detections thus firmly imply that these galaxies do not host AGNs with luminosities comparable to the weakest known in any galaxy.

There are a number of MIR diagnostics used to characterize the dominant ionizing radiation field in galaxies. Since the flux ratio of emission lines from high-ionization to low-ionization ions depends on the nature of the ionizing source, the [NeV] $14.3 \mu\text{m}$ /[NeII] $12.8 \mu\text{m}$ and the [OIV] $25.9\mu\text{m}$ /[NeII] $12.8\mu\text{m}$ line flux ratios have been widely used to characterize the nature of the dominant ionizing source in galaxies (Genzel et al. 1996; Sturm et al. 2002; Satyapal et al. 2004; Dale et al. 2006,2009). We can compare our line flux ratio upper limits to the ratios in standard AGNs. Again, using the recent compilations of MIR line fluxes of standard AGNs observed by *Spitzer* from Deo et al. (2007), Tommasin et al. (2008), and Dale et al. (2009), there are 56 AGNs with measured [NeII] $12.8\mu\text{m}$ and [NeV] $14\mu\text{m}$ line fluxes. The [NeV]/[NeII] line flux ratio in these galaxies ranges from 0.02 to 2.97, with a median value of 0.73. As can be seen from Table 4, all of the galaxies with [NeV] $14.3 \mu\text{m}$ upper limits have [NeV]/[NeII] upper limits well below the median value in standard AGNs, supporting the hypothesis that these galaxies lack an AGN. Similarly, using the fluxes compiled in Verma et al. (2003), Deo et al. (2007), Tommasin et al. (2008), Dale et al. (2009), and Melendez et al. (2008), there are over 100 AGNs with measured [NeII] $12.8\mu\text{m}$ and [OIV] $25.9 \mu\text{m}$ line fluxes. The [OIV]/[NeII] line flux ratio in these galaxies ranges from 0.02 to 11.1, with a median value of 1.33. As can be seen from Table 4, the upper limits for the [OIV]/[NeII] flux ratio in our sample are also all well below the median value in standard AGNs, again strongly suggesting that these galaxies lack AGN.

² Note that a few of the AGN were observed more than once. In such cases, we always selected measurements that were obtained with the high resolution IRS module, choosing the reference with the largest compilation.

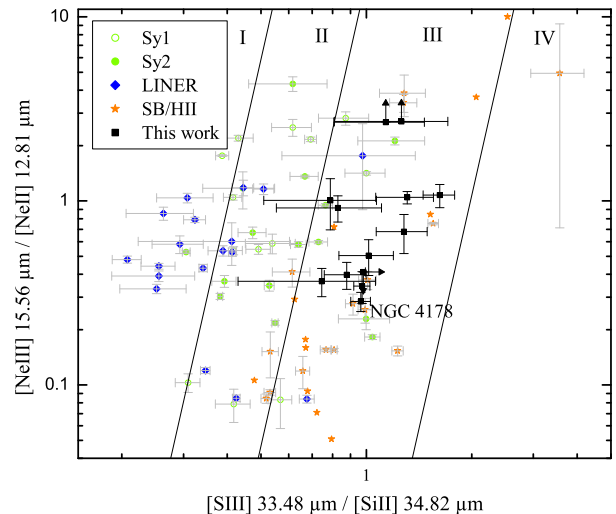


FIG. 4.— Mid-infrared diagnostic diagram used to separate AGNs from starbursts and "HII" galaxies from Dale et al. (2006). Galaxies included are from Dale et al. (2009), Tommasin et al. 2008, Verma et al. (2003), and our sample of bulgeless galaxies, which are indicated by the filled squares. Regions I-IV are delineated by the solid line, as proposed by Dale et al. 2006, demonstrating that no known AGNs fall in regions III and IV, where all of our bulgeless galaxies are located.

An alternative diagnostic proposed by Dale et al. (2006) to classify the ionizing source in galaxies involves the [NeIII] $15.5\mu\text{m}$ /[NeII] $12.8 \mu\text{m}$ flux ratio and the [SIII] $33.48\mu\text{m}$ / [SiII] $34.82\mu\text{m}$ flux ratio. They find that AGNs display lower [SIII] $33.48\mu\text{m}$ /[SiII] $34.82\mu\text{m}$ line flux ratios than "pure star-forming" nuclei, presumably due to enhanced [SiII] emission in X-ray dominated regions around AGNs (Maloney et al. 1996). In Figure 4 we plot the [NeIII] $15.5\mu\text{m}$ /[NeII] $12.8 \mu\text{m}$ flux ratio versus the [SIII] $33.48\mu\text{m}$ /[SiII] $34.82\mu\text{m}$ flux ratio for standard AGN, starburst and HII galaxies (based on the compilations listed above), and for those galaxies in our sample for which the lines were detected. We delineate the four regions defined by Dale et al. (2006), where regions I and II are exclusively occupied by LINERs and Seyferts, and regions III and IV are exclusively occupied by HII nuclei and extranuclear HII regions. As can be seen, all of the galaxies in our sample (including NGC 4178) fall entirely within region III, exhibiting similar ratios to HII nuclei.

To summarize, with the exception of NGC 4178, the MIR spectra of all our sample galaxies strongly suggest that they do not contain AGN.

4.3. Density of the Ionized Gas

Abundance-independent density estimates have been obtained using infrared fine-structure transitions from like ions in the same ionization state with different critical densities. The density diagnostic available in the IRS spectra of our objects are the [SIII] $18.71\mu\text{m}$ and $33.48 \mu\text{m}$ lines (where $n_{crit} \sim 1.5 \times 10^4 \text{ cm}^{-3}$, and $4.1 \times 10^3 \text{ cm}^{-3}$, respectively, where $n_{crit} = A_{ul}/\gamma_{ul}$, with A_{ul} the Einstein A coefficient and γ_{ul} the rate coefficient for collisional de-excitation from the upper to the

Table 4: [NeV] Luminosity Upper Limits and Line Flux Ratios

| Name | $L_{[\text{NeV}]}$ | $[\text{OIV}]_{25.89}/[\text{NeII}]_{12.81}$ | $[\text{NeV}]_{14.32}/[\text{NeII}]_{12.81}$ | $[\text{SIII}]_{18.71}/[\text{SIII}]_{33.48}$ |
|---------|--------------------|--|--|---|
| IC2574 | <2.52 | ... | ... | ... |
| NGC2500 | <5.77 | ... | ... | ... |
| NGC2537 | <3.12 | <0.91 | <0.35 | ... |
| NGC3027 | <2.06 | <0.46 | <0.08 | 1.67 |
| NGC3432 | <2.55 | <0.29 | <0.13 | 1.91 |
| NGC3495 | <3.48 | <0.44 | <0.14 | 1.56 |
| NGC4145 | <3.09 | <0.27 | <0.08 | 0.51 |
| NGC4242 | <2.21 | ... | ... | ... |
| NGC4496 | <6.94 | ... | ... | ... |
| NGC4618 | <2.88 | <0.26 | <0.13 | 3.59 |
| NGC4656 | <2.05 | <0.18 | <0.09 | 1.54 |
| NGC4713 | <6.72 | <0.15 | <0.12 | 1.90 |
| NGC5147 | <5.28 | <0.27 | <0.11 | 1.43 |
| NGC5204 | <2.35 | ... | ... | 0.95 |
| NGC5585 | <1.13 | <0.69 | <0.18 | 1.22 |
| NGC6689 | <5.28 | ... | ... | ... |
| NGC784 | <4.48 | ... | ... | ... |
| NGC959 | <4.25 | ... | ... | ... |

Columns Explanation: Col(1): Common Source Names; Col(2): [NeV] 14.32 μm luminosity 3σ upper limits in units of 10^{37} ergs s^{-1} ; Col(3) & (4) & (5): Line flux ratios using fluxes from full apertures listed in Table 3.

lower level). The results are largely unaffected by the shape of the ionizing continuum. However, in Dudik et al. (2007), we showed that since the [SIII] emission is generally extended and the LH slit is larger than the SH slit, any analysis derived using line fluxes obtained from apertures of different sizes is ambiguous for most nearby galaxies. Furthermore, differential extinction towards the emitting gas in very obscured sources will also affect the line flux ratio, resulting in further ambiguities in the interpretation of the ratio. Nonetheless, for comparative purposes, we list in Table 4 the [SIII] $_{18.71}$ μm /[SIII] $_{33.48}$ μm line flux ratios for our sample of galaxies. From Table 4, we see that for the galaxies in which both lines are detected, the line flux ratio ranges from 0.5 to 3.6, with an average value of 1.6. As shown in Dudik et al. (2007), at the distances for most of our sources, the [SIII] emission will likely extend beyond the SH aperture, resulting possibly in an artificially *lower* [SIII] $_{18.71}$ μm /[SIII] $_{33.48}$ μm line flux ratio. As a comparison, the *aperture-matched* [SIII] $_{18.71}$ μm / [SIII] $_{33.48}$ μm line flux ratio in the SINGS sample of 75 galaxies from Dale et al. (2009) ranges from 0.3 to 2, with an average value of 0.8, significantly *lower* than the values listed in Table 4. Indeed, 97% of the SINGS sample has line flux ratios below the average value found in our sample. Since aperture affects should in principle lower the line flux ratios in our sample compared to the aperture-matched values in Dale et al. (2009), the higher [SIII] $_{18.71}$ μm /[SIII] $_{33.48}$ μm line flux ratios found in our sample of bulgeless galaxies possibly implies higher gas densities toward the [SIII]-emitting gas. The gas densities derived using the models from Dudik et al. (2007) for a gas temperature of $T = 10^4$ K (obtained using the collision strengths from Tayal & Gupta (1999) and radiative transition probabilities from Mendoza & Zeppen 1982) range from $\sim 100 \text{ cm}^{-3}$ - $3 \times 10^3 \text{ cm}^{-3}$ for our sample. We emphasize that the ambiguities inherent in the use of the [SIII] ratio, particularly significant in nearby galax-

ies, preclude us from making definitive statements about the actual gas densities in the ionized gas in our sample. Nevertheless, the [SIII] ratios appear to imply higher ionized gas densities compared with standard AGN and normal/starburst galaxies of earlier Hubble type. We note that Dale et al. (2009) find that the average [SIII] ratios is independent of whether the region probed is a star-forming or AGN environment.

5. THE AGN IN NGC 4178

5.1. Line Fluxes and Spectral Line Fits

In Figure 5, we show the spectra extracted from the full SH aperture near 13 μm , 14 μm , and 15 μm , showing three emission lines from different ionization states of Neon. As can be seen, there is a clear detection ($\sim 6\sigma$) of the [NeV] 14.32 μm line, providing strong evidence for an AGN in this galaxy. The [NeV] line is not resolved with the R=600 *Spitzer* SH spectral resolution. The [NeV]/[NeII] line flux ratio for NGC 4178 is 0.12, within the range but at the low end of the values observed in standard AGNs as discussed above. The [NeV]/[NeII] line flux ratio in NGC 4178 is a factor of ~ 2 higher than the same ratio in NGC 3621, our previously discovered Sd galaxy with [NeV] emission. The infrared spectra (S07, Abel & Satyapal 2008) together with newly acquired additional multiwavelength observations (Barth et al. 2009; Gliozzi et al. 2009) have made the case for an AGN in NGC 3621 secure. It is thus very likely that NGC 4178 also harbors an AGN, and that it is possibly slightly more energetically significant than the one in NGC 3621. The upper limit to the [OIV]/[NeII] line flux ratio in NGC 4178 is 0.1, still within range of the observed values in standard AGNs as discussed above. As in the case of NGC 3621, the low [NeV]/[NeII] and [OIV]/[NeII] line flux ratios in NGC 4178 suggests that the *Spitzer* spectrum is dominated by regions of star formation, and that there is significant contamination of the lower ionization emission lines from star formation

within the *Spitzer* aperture.

The [NeV] 14.32 μm luminosity observed from NGC 4178 is 8.23×10^{37} ergs s^{-1} , slightly higher than the value observed in NGC 3621 (5×10^{37} ergs s^{-1} ; S07) and almost 3 orders of magnitude lower than the median value observed in standard AGNs (see Section 3.1.1). It is also on the low end of the luminosities observed in other recently discovered late-type galaxies showing [NeV] emission presented in S08. Like NGC 3621, NGC 4178 likely harbors a very weak AGN.

5.2. Other Evidence

There does not appear to be any previously published evidence for an AGN in NGC 4178. This source was not observed by *Chandra* or *XMM-Newton*. The galaxy was not detected by Einstein and the upper limit to the X-ray luminosity, ($L_X \sim 2.5 \times 10^{40}$ ergs s^{-1} ; Fabbiano, Kim, & Trinchieri 1992) is consistent with a low luminosity AGN (e.g. Ho et al. 2001, Dudik et al. 2005). There is no evidence of a central source at radio wavelengths. The radio emission at 2.8, 6.3 and 20 cm peaks 55 " away from the optical center, and is associated with optically bright knots (Niklas et al. 1995a). There is no evidence of an excess in the radio-FIR correlation as is seen in AGN (Niklas et al. 1995b) and the radio spectral index is typical of star forming galaxies (Vollmer et al. 2004). The [NeV] detection reported in this work is the first observation suggesting the presence of an AGN.

In Abel & Satyapal (2008), we used the spectral synthesis code CLOUDY to model the emission line spectrum from gas ionized by both an input AGN radiation field and a young starburst. In the case of NGC 3621, we showed that the MIR spectrum cannot be replicated unless 30-50% of the bolometric luminosity within the *Spitzer* IRS aperture is due to an AGN. In Figure 6, we show the predicted [NeV]14.3 μm /[NeII]12.8 μm flux ratio versus the [OI]/ $H\alpha$ and [SII]/ $H\alpha$ optical line flux ratios based on the models from Abel & Satyapal (2008) for varying values of the ionization parameter (U; the dimensionless ratio of ionizing flux to gas density) and AGN luminosity contribution. We display only a narrow range of ionization parameters that generate line flux ratios within the range observed in NGC 4178 and NGC 3621. A more extensive grid of theoretical calculations, with all standard optical line flux ratios plotted, is presented in Abel & Satyapal (2007). As can be seen from Figure 6, the MIR and optical emission line spectra of NGC 4178 cannot be replicated with a pure starburst ionizing radiation field. An AGN contribution of ~ 30 -90% is required.

Although it is clear that gas photoionized solely by even the youngest starburst ionizing radiation field cannot simultaneously reproduce the optical and mid-infrared spectrum of NGC 4178, the possibility that the [NeV] emission originates from shocked gas associated with a starburst-driven superwind (e.g. Veilleux, Cecil, & Bland-Hawthorn 2005) needs to be explored. Since the large aperture of the *Spitzer* IRS modules precludes us from using morphological arguments to rule out shocks, we consider whether the combined optical and mid-infrared fine structure line ratios are consistent with radiative shock models. Using the extensive grid of models from the most recent MAPPINGS III shock and photoionization code (Allen et al. 2008), we find that the

optical spectrum of NGC 4178 cannot be reproduced for most of the parameter space they studied. In fact, the only shock models which can simultaneously reproduce the observed [O III]/ $H\beta$, [N II]/ $H\alpha$, and [S II]/ $H\alpha$ line ratios for NGC 4178 are for high-density ($n(\text{H}) = 1000$ cm^{-3}) shocks (Allen et al. 2008; Figure 22a). However, at these densities, the mid-infrared spectrum, in particular the [Ne III]/[Ne II] is 1-2 orders of magnitude higher than the observed value of 0.28 for NGC 4178. Thus, the mid-infrared spectrum and the optically "normal" spectrum of NGC 4178 cannot be simultaneously replicated by any shock model. Although high density radiative shocks may play a role in the emission line spectrum of NGC 4178 (and other AGN), it appears that the combined optical and mid-infrared spectrum cannot be produced without an AGN radiation field. Follow-up *Chandra* observations are crucial to confirm the presence of the AGN and constrain its location.

5.3. Bolometric Luminosity and Black Hole mass limit

We can obtain an order of magnitude estimate of the bolometric luminosity of the AGN in NGC 4178 using the [NeV] line luminosity. Assuming that the line emission arises exclusively from the AGN, we follow the procedure adopted by S07 and S08 to estimate the nuclear bolometric luminosity of the AGN. Using the tight correlation between the [NeV] 14 μm line luminosity and the AGN bolometric luminosity found in a large sample of standard AGN (Equation 1 in S07), the AGN bolometric luminosity of NGC 4178 is $\sim 8 \times 10^{41}$ ergs s^{-1} , slightly greater than the estimate for the AGN bolometric luminosity of NGC 3621 (S07). This estimate assumes that the relationship between the [NeV] 14 μm line luminosity and the bolometric luminosity established in more luminous AGN (see S07) extends to the lower [NeV] luminosity range characteristic of NGC 4178 and other late-type galaxies. The nuclear bolometric luminosities of the AGNs discovered in the late-type galaxies from S08 range from $\sim 3 \times 10^{41}$ ergs s^{-1} to $\sim 2 \times 10^{43}$ ergs s^{-1} , with a median value of $\sim 9 \times 10^{41}$ ergs s^{-1} . As can be seen, the luminosity of the AGN in NGC 4178 is typical of other recently discovered AGN in low-bulge galaxies.

If we assume that the AGN is radiating below the Eddington limit, we can estimate the lower limit to the mass of the black hole based on the AGN bolometric luminosity estimate. The Eddington mass estimate in NGC 4178 is $\sim 6 \times 10^3 M_\odot$, well within the range of lower mass limits found in other late-type galaxies with AGN (S07, S08). There appears to be a nuclear star cluster in NGC 4178 (see section 7.1). However, there are no measurements of the central velocity dispersion. We therefore cannot determine if the lower mass limits derived for the black hole mass are incompatible with the M_{BH} - σ relation, assuming a linear extrapolation to the low mass range.

5.4. Comparison to other AGNs in Bulgeless Galaxies

NGC 4178 is one of less than a handful of completely bulgeless disk galaxies showing evidence for an AGN. The best-studied definitively bulgeless disk galaxy with an AGN is the galaxy NGC 4395, which shows the hallmark signatures of a type 1 AGN (e.g. Filippenko & Ho 2003; Lira et al. 1999; Moran et al. 1999). The bolometric luminosity of the AGN is $\sim 10^{40}$ ergs s^{-1} (Filippenko

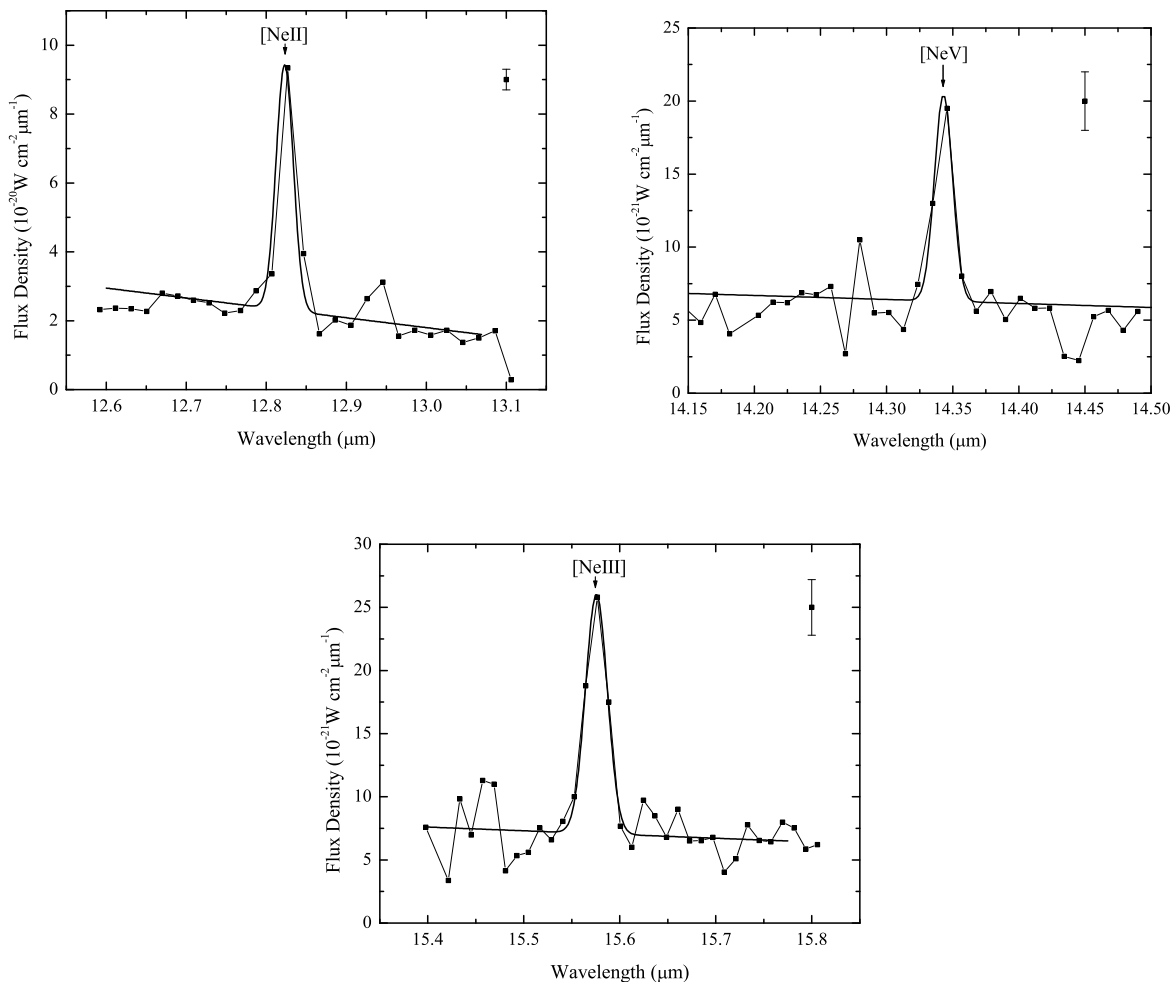


FIG. 5.— IRS SH spectra of NGC 4178 showing the detections of the [NeII] 12.81 μm , [NeV] 14.32 μm , and [NeIII] 15.56 μm fine structure lines. Representative error bars are displayed in the upper right corner of each plot.

& Ho 2003), almost two orders of magnitude lower than the estimated bolometric luminosity of the AGN in NGC 4178. The estimated bolometric luminosity of the AGN in NGC 3621 is a factor of 1.6 less (S07) than that of the AGN in NGC 4178, making NGC 4178 the most luminous AGN in an Sd galaxy currently known. The black hole mass of NGC 4395, determined by reverberation mapping, is $M_{BH} = (3.6 \pm 1.1) \times 10^5 M_{\odot}$ (Peterson et al. 2005). This value for the black hole mass would be consistent with the lower limit of the black hole mass derived for NGC 4178 of $6 \times 10^3 M_{\odot}$ if the AGN is accreting at a high rate. Our recent X-ray observations, when combined with our *Spitzer* observations, suggest that the black hole mass in NGC 3621 is $\sim 2 \times 10^4 M_{\odot}$ and that it is accreting at a high rate ($L_{bol}/L_{Edd} > 0.2$) (Glozzi et al. 2009). If NGC 4178 is similar to NGC 3621, then its black hole mass is comparable to that in NGC 4395 and is inline with those inferred for nuclear black holes in other pseudobulge galaxies (Greene & Ho 2007).

6. MID-INFRARED AGN DETECTION RATE IN SD GALAXIES

In S08, we showed that optical studies significantly miss AGN in late-type galaxies. From the H97 sample, out of the full sample of 486 galaxies, 207 are of Hubble type Sbc or later, and only 16 (8%) are optically classified as AGN. Using MIR diagnostics, we demonstrated that the AGN detection rate in optically normal disk galaxies of Hubble Type Sbc or later, is $\sim 30\%$, implying that the overall fraction of late-type (Sbc or later) galaxies hosting AGNs is possibly more than 4 times larger than what optical spectroscopic studies indicate. Although it is now clear that AGNs do reside in a significant number of late-type galaxies, virtually all of the newly discovered AGNs are in galaxies with Hubble type of Scd or earlier. Prior to the current work, there were only a handful of Sd galaxies observed by the high resolution modules of *Spitzer's* IRS, precluding us from determining based on MIR diagnostics the true AGN fraction in galaxies with essentially *no* bulge.

In Figure 7, combining our current sample with that from S08, we show the AGN detection fraction in optically normal galaxies as a function of Hubble type. Since

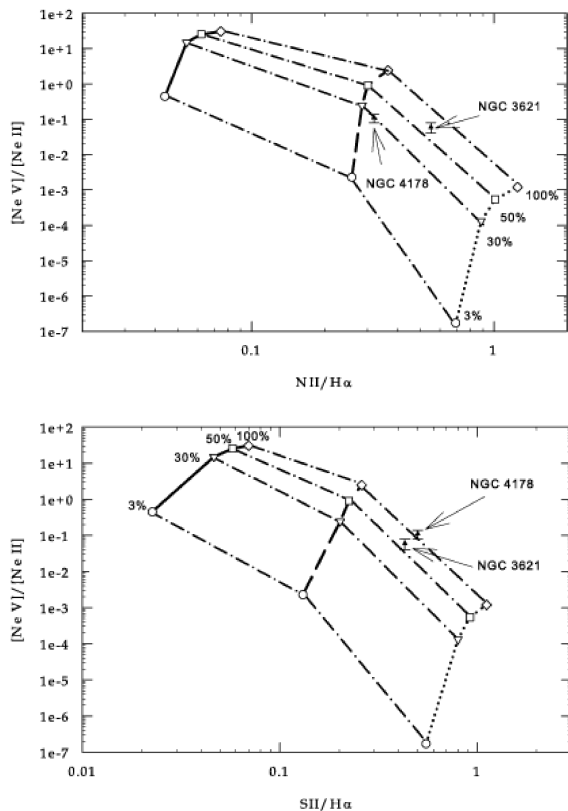


FIG. 6.— The $[\text{NeV}]14.3\mu\text{m}/[\text{NeII}]12.8\mu\text{m}$ line flux ratio versus the optical (a) $[\text{NII}]/\text{H}\alpha$ flux ratio and (b) the $[\text{SII}]/\text{H}\alpha$ flux ratio from the models from Abel & Satyapal (2008). The solid, dashed, and dotted line display model results for ionization parameters of -1.5 , -2.5 , and -3.5 , respectively. The dashed-dotted lines show the fraction of the total luminosity due to the AGN. The line attached to the circles represent 3% AGN, inverted triangles 10% AGN, squares 30% AGN, diamond 50% AGN, and triangles 100% AGN, as indicated in the Figure. The line flux ratios for NGC 4178 and NGC 3621 are shown. We note that the optical line flux ratios for NGC 4178 are taken directly from Table 4 in H97. The $[\text{NII}]/\text{H}\alpha$ flux ratio for NGC 3621 is taken from the large aperture ($20'' \times 20''$) measurements from Dale et al. 2006. The $[\text{SII}]/\text{H}\alpha$ measurement for NGC 3621 is from the higher spatial resolution ($1''$) observations from Barth et al. (2009).

the sensitivity of the observations varied across the sample, we also indicate with a downward arrow in Figure 6 the number of galaxies with $[\text{NeV}] 14 \mu\text{m}$ 3σ line sensitivity of $10^{38} \text{ ergs s}^{-1}$ or better. As can be seen, all of the Sd/Sdm galaxies were observed with the highest sensitivity. There are a total of 22 Sd/Sdm galaxies observed by *Spitzer* IRS and only 1 with a $[\text{NeV}]$ detection (NGC 4178). Figure 7 shows that the AGN detection rate in optically normal galaxies drops dramatically for pure disk galaxies, with a detection rate of only 4.5%. From the H97 sample, out of the full sample of 486 galaxies, excluding interacting and irregular galaxies, 26 are of Hubble type Sd/Sdm and only one is optically identified as an AGN (NGC 4395). With the discovery of only one additional AGN in an Sd galaxy from the H97 sample based on MIR diagnostics, the overall detection rate of AGN in pure disk galaxies is only $\sim 8\%$, significantly lower than the detection rate in late-type galaxies

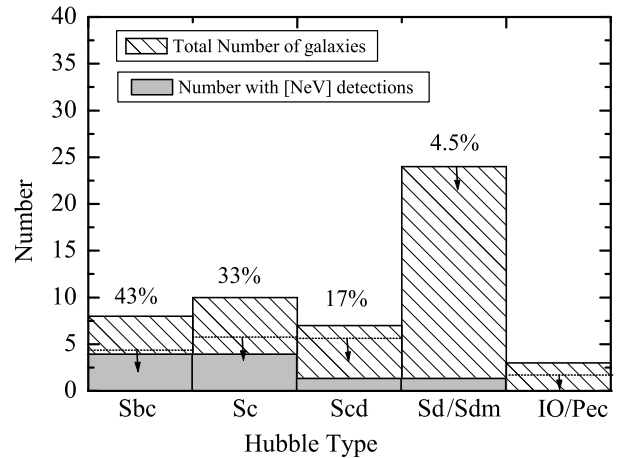


FIG. 7.— The distribution of Hubble types for the current sample combined with that from S08. The galaxies with $[\text{NeV}]$ detections are indicated by the filled histogram. Since the sensitivity of the observations varied across the sample, we also indicate with a downward arrow in Figure 6 the number of galaxies with $[\text{NeV}] 14 \mu\text{m}$ line sensitivity of $10^{38} \text{ ergs s}^{-1}$ or better. As can be seen the AGN detection rate in optically normal galaxies drops dramatically for galaxies with no bulge component.

with some bulge component. Our study thus shows that AGNs in pure disk galaxies do not appear to be hidden but are indeed truly rare.

7. DEMOGRAPHICS OF LATE-TYPE GALAXIES WITH AGNS

7.1. A Nuclear Star Cluster in NGC 4178?

With the discovery of an AGN in NGC 4178, there are now only 3 known AGN in Sd galaxies. As mentioned earlier, the two other Sd galaxies with AGNs, NGC 4395 and NGC 3621, both have prominent NSCs. In Figure 8, we show the *HST* NICMOS image of NGC 4178 (Böker et al. 1999). The image reveals a prominent source close to the apparent photocenter, indicated by an arrow. As will be discussed in Section 8, the luminosity of this source is consistent with that of a NSC. Unfortunately, the NICMOS image is not centered well, and thus does not allow an unambiguous determination of the photocenter.

However, visual inspection and a cursory isophote analysis over the limited NICMOS field of view suggest that the location of the NSC is indeed consistent with that of the photocenter of NGC 4178. Because the spatial resolution of the *Spitzer* data precludes us from determining the spatial location of the $[\text{NeV}]$ peak to determine whether it coincides with the NSC, follow-up *Chandra* observations are crucial to confirm that the AGN indeed resides within the putative NSC. If we assume for the moment that the prominent central source in the NICMOS image is a NSC, then one can infer that all known AGNs in Sd galaxies reside in NSCs, possibly suggesting that in the absence of any bulge, an NSC is required for an AGN to be present.

We can estimate a rough mass for the NSC in NGC 4178 if we assume the average I-band M/L ratio for NSCs in late-type galaxies with measured dynamical masses (Walcher et al. 2005). Based on the rough I-band mag-

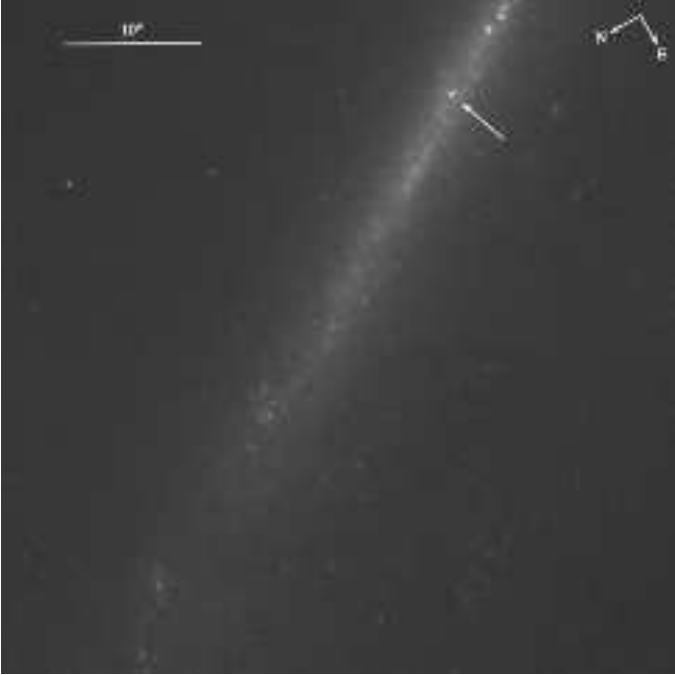


FIG. 8.— *HST* NICMOS H-band image of NGC 4178. The location of the NSC is indicated by the arrow and is consistent with the apparent photocenter. The field of view of the image is $51'' \times 51''$.

nitude estimate (see Section 8), the nuclear cluster mass in NGC 4178 is $\sim 0.5 \times 10^6 M_{\odot}$, comparable to the nuclear cluster mass in NGC 4395 (Seth et al. 2008) and an order of magnitude less than the one in NGC 3621 (Barth et al. 2009). Seth et al. (2008) find that in cases with known nuclear cluster and black hole masses, the ratio of the black hole mass to nuclear cluster mass, M_{BH}/M_{NC} , ranges from 0.1-1. This ratio is $\sim 1/3$ in NGC 4395. Using the lower limit to the black hole mass for NGC 4178, we find $M_{BH}/M_{NC} > 10^{-2}$, which is possibly consistent with the ratio found in galaxies with measured nuclear cluster and black hole masses (Seth et al. 2008).

7.2. AGNs in Late-type Bulges

It is well established that AGN are common in early-type galaxies and that there is a trend of increasing AGN activity with bulge mass (e.g. H97; Kauffman et al. 2003). Based on our study and other recent studies, it is also now clear that AGN do exist in late-type galaxies that lack a classical bulge and that they are significantly more common than previously thought (S07; S08; Greene, Ho, & Barth (2009); Shields et al. 2008; Ghosh et al. 2008; Barth et al. 2008; Dewangan et al. 2008; Desroches & Ho 2009). Late-type galaxies are often characterized by so-called pseudobulges, with exponential surface brightness profiles similar to disks rather than classical bulges. These pseudobulges are thought to have formed from quiescent secular processes within the host galaxy, in contrast to the violent merger-driven events thought to have formed classical bulges (see review in Kormendy & Kennicutt 2004). It is therefore relevant to ask whether the incidence and properties of BHs in late-type galaxies are related to the presence and properties of pseudobulges.

Combining the samples from S08, and including NGC 3621 (S07), and this work, there are a total of 52 nearby optically normal late-type galaxies in which the presence or absence of AGN has been determined by MIR diagnostics. With a total of 9 AGN in this combined sample, we can attempt to investigate the relationship between AGN activity and the host galaxy properties for galaxies of Hubble type Sbc or later. We emphasize, that the AGNs in this sample were previously unknown based on optical spectroscopic studies. The study of the demographics of these newly discovered AGNs allows us to investigate whether there are any trends in AGN activity with host galaxy properties in late-type galaxies that were previously unseen in studies based on optical observations.

For those 13 galaxies in our current sample with existing *HST* imagery, we have used the archival *HST* data to establish the presence or absence of a nuclear star cluster (see Table 1). None of these *HST* images show any evidence for a bulge component, confirming our selection criterion, and we therefore assume the remaining 5 galaxies in our sample are bulgeless as well. For the remaining galaxies in our combined *Spitzer* sample, we searched the literature for all information on the structural properties of the host galaxies. Of the 52 late-type galaxies, 32 had published surface brightness profile fits to characterize the bulge properties (Knapen et al. 2003; Laurikainen et al. 2004; Scarlata et al. 2004; Dong & De Robertis 2006; Drory & Fisher 2007). We point out that several of the published bulge properties are based on ground-based imagery with low spatial resolution, which can significantly compromise the inferred bulge parameters. In addition, the presence or absence of NSCs has not been investigated in all galaxies. We therefore do not carry out a quantitative analysis of the relationship between bulge parameters and AGN presence and properties. Instead, we investigate whether there are any evident *trends* between the host galaxy properties and the incidence of AGN activity. Most of the galaxies in our previous sample (S08) have pseudobulges or weak classical bulges and four have identified NSCs. We point out that the NSC presence has not been investigated in the majority of galaxies in the sample and it is likely that most of these late-type galaxies do have NSCs. Of the 8 AGNs in our S08 sample, 6 have published surface brightness profile fits. Amongst these sources, 2 are reported to have classical bulges (NGC 3367, NGC 4414; Dong & De Robertis 2006, Laurikainen et al. 2004, respectively), and the remaining 4 are reported to have surface brightness profiles consistent with pseudobulges (NGC 3938, NGC 4321, NGC 4536, and NGC 5055; Dong & De Robertis 2006, Scarlata et al. 2004, Drory & Fisher 2007). One of the AGN galaxies is reported in the literature to host a NSC (NGC 4321; Knapen et al. 1995), but the presence or absence of a NSC in the remaining AGN galaxies has not been established. Although the small sample size and the ambiguity in the published bulge properties precludes us from conducting a quantitative investigation of the relationship between bulge parameters and nuclear cluster presence and AGN activity, it appears that most AGNs in late-type galaxies reside in galaxies with pseudobulges or weak classical bulges. It is also clear that NSCs and AGNs coexist, consistent with the findings from Seth et al. (2008) in more massive

galaxies spanning a wide range of Hubble types.

Most importantly, our current study robustly shows that AGNs are extremely rare in bulgeless galaxies and that for the few cases where one does exist (NGC 3621, NGC 4178, and NGC 4395), there is a prominent NSC. These findings possibly suggest that if there is no bulge of any kind in a galaxy, the galaxy *must have a NSC* in order to host an AGN.

8. IS NGC 4178 SPECIAL?

Our findings demonstrate that AGN are truly rare in bulgeless galaxies. An important question to then ask is what distinguishes bulgeless disk galaxies *with* AGN from those *without* AGN? Is the presence and properties of the black hole in any way related to the properties of the host galaxies in cases where there truly is *no* bulge? With 18 bulgeless disk galaxies in our sample and only one AGN (NGC 4178), the question arises whether NGC 4178 is in some way special in our sample. Of course the absence of an AGN does not imply the absence of a quiescent massive black hole in any of the galaxies in our sample. The only dynamical study that rules out the presence of a massive black hole ($M_{BH} < 1500 M_{\odot}$) in a bulgeless disk galaxy was carried out for the nearby galaxy M33 (Gebhardt et al. 2001).

We investigated whether NGC 4178 is unique in any way in its basic host galaxy properties listed in Table 1. The total estimated galaxy mass for NGC 4178 is $\sim 10^8 M_{\odot}$, on the high end but not the highest of the galaxies in our sample (see Figure 1). From Table 1, we can see that the estimated HI mass is high but again comparable to or lower than several other galaxies in the sample, implying that the disk mass does not appear to be related to the presence or absence of an AGN in bulgeless disk galaxies. Similarly, the inclination-corrected HI rotational amplitude of NGC 4178 is high but not the highest in the sample (see Table 1), suggesting that the total dark matter mass is not the determining factor in whether or not a bulgeless disk galaxy hosts an AGN. Finally the nuclear SFR in NGC 4178 listed in Table 1, estimated using the extinction-corrected H α luminosity, is only slightly larger than the median value for the entire sample, but well below the highest value in the sample. There is thus no clear indication that the basic host galaxy properties in NGC 4178 are exceptional in any way compared to the rest of our sample.

If the basic host galaxy properties in NGC 4178 do not distinguish themselves from the rest of sample, we can ask whether the nuclear cluster properties do. Using the *HST* NICMOS image of NGC 4178, we estimate a magnitude of $m_H=18.24$ using a circular aperture of 3 pixels centered on the putative NSC. We point out that in this analysis, we are assuming that the AGN in NGC 4178 is coincident with the putative NSC - an assumption which is not possible to confirm with the poor spatial resolution of the *Spitzer* data. Follow-up high spatial resolution *Chandra* observations are crucial to confirm this hypothesis. Using the latest stellar population synthesis models from Bruzual & Charlot (2009), the I-H color for single age population older than 10^8 years, assuming solar metallicity and a Chabrier (2003) initial mass function does not exceed 1.7. This means that the nuclear cluster in NGC 4178 has an absolute I-band magnitude of $M_I \sim -11$, typical of the I-band magnitudes of nuclear clusters

in the extensive sample of nuclear clusters in late-type galaxies from Böker et al. (2002) (see their Figure 5). We note that we have not made any extinction correction, which could be significant in an edge-on galaxy such as NGC 4178. We also assumed an old stellar population. Since NGC 4178 shows prominent low ionization emission lines indicating the presence of young stars, the nuclear cluster color might be bluer than assumed above, resulting in an underestimate of the I-band luminosity. Finally, since the AGN is weak and hidden at optical wavelengths, we have assumed that the AGN contribution to the central luminosity in the H-band is negligible. Our estimate of the nuclear cluster luminosity should therefore be considered approximate. However, it does appear based on this rough estimate, that the nuclear cluster luminosity in NGC 4178 is typical of a nuclear cluster in late-type galaxies. There is thus no clear indication that NGC 4178 distinguishes itself from the rest of our sample of disk galaxies both in terms of the overall galaxy properties or its nuclear cluster luminosity. The recipe for forming and growing a massive black hole in a truly bulgeless disk galaxy is still unknown.

9. SUMMARY AND CONCLUSION

We conducted a MIR spectroscopic investigation of 18 completely bulgeless disk galaxies showing no signatures of AGN in their optical spectra in order to search for low luminosity and/or embedded AGN. This is the first systematic search for weak or hidden AGN in a statistically significant sample of essentially bulgeless disk galaxies. The primary goal of our study was to determine the incidence of AGNs in galaxies in the absence of a significant bulge. Our high resolution *Spitzer* spectroscopic observations reveal that while AGNs in galaxies with pseudobulges or weak classical bulges are significantly more common than once thought, AGNs in truly bulgeless disk galaxies are exceedingly rare. Our main results are summarized below:

1. We detected the high ionization [NeV] 14.3 μm emission line in only one out of the 18 galaxies in the sample, providing strong evidence for an AGN in this one source. This galaxy, NGC 4178, is a nearby ($d=16.8$ Mpc) edge-on disk galaxy with optical emission line ratios in the normal star formation regime, indicating that there is absolutely no hint of an AGN based on its optical spectrum.
2. With the exception of NGC 4178, none of the galaxies in the sample shows any evidence in the MIR for a weak or embedded AGN, suggesting that they lack AGN. Instead, most galaxies show signs of active star formation and possibly higher ionized gas densities than galaxies of earlier Hubble type.
3. Our work suggests that the AGN detection rate based on MIR diagnostics in late-type optically normal galaxies is high (30-40%) in galaxies of Hubble type Sbc and Sc but drops drastically in Sd/Sdm galaxies (4.5%). Our observations confirm that AGNs in completely bulgeless disk galaxies are not hidden in the optical but truly are rare.
4. The AGN bolometric luminosity of NGC 4178 inferred using our [NeV] line luminosity is $\sim 8 \times 10^{41}$

ergs s⁻¹, a factor of 1.6 times greater than the estimated bolometric luminosity in the Sd galaxy NGC 3621, and almost two orders of magnitude greater than the AGN bolometric luminosity of NGC 4395, the best-known AGN in an Sd galaxy. This makes the AGN in NGC 4178 the most luminous known in a bulgeless disk galaxy. Assuming that the AGN is radiating below the Eddington limit, this corresponds to a lower mass limit for the black hole of $\sim 6 \times 10^3 M_{\odot}$. There are no published measurements of the central stellar velocity dispersion. It is therefore unknown if the lower mass limit for the black hole in NGC 4178 violates the $M_{\text{BH}}-\sigma$ relation established in early-type galaxies.

5. NGC 4178 is now one of only 3 known Sd galaxies showing evidence for an AGN. *HST* images of this galaxy suggests that it has a prominent NSC, similar to the ones seen in the other two known Sd galaxies with AGNs (NGC 3621, NGC 4395). If follow-up *Chandra* observations confirm that the AGN is coincident with the putative NSC in this source, this finding suggests that if there is *no* bulge of any kind in a galaxy, the galaxy must have a NSC in order to host an AGN.
6. We find that NGC 4178 is not exceptional in our sample of 18 bulgeless galaxies based both on its basic host galaxy properties (galaxy mass, disk mass, dark matter halo mass, nuclear SFR) and

nuclear cluster properties. The recipe for forming and growing a black hole in a truly bulgeless disk galaxy still remains a mystery.

It is a pleasure to thank Rachel Dudik for her invaluable help in consulting with us on data analysis issues, for troubleshooting various software installation roadblocks, for her technical assistance in planning the observations, and for stimulating science discussions. This work would not have been possible without her expertise in IRS data analysis. We are also very grateful to the *Spitzer* helpdesk for numerous emails in support of our data analysis questions. Brian O'Halloran and Dan Watson were very helpful in consulting with us on data analysis procedures. This work is based on observations taken with the *Spitzer* Space Telescope, which is operated by JPL/Caltech under a contract with NASA. The thoughtful suggestions of the anonymous referee helped improve this paper. We are also very grateful for a fruitful discussion with Dave Alexander and Andy Goulding, which led us to outline more explicitly our data analysis procedure in Section 3. This research has made use of the NASA/IPAC Extragalactic Database (NED), which is operated by the Jet Propulsion Laboratory, California Institute of Technology, under contract with the National Aeronautics and Space Administration. SS gratefully acknowledges financial support from NASA grant RSA 1345391.

REFERENCES

- Abel, N.P. & Satyapal, S. 2008, ApJ, 678, 686
 Allen, M.G., Groves, B. A., Dopita, M. A., Sutherland, R. S., Kewley, L. J. 2008, ApJS, 178, 20
 Armus, L., Charmandaris, V., Bernard-Salas, J., Spoon, H. W. W., et al. 2007, ApJ, 656, 148
 Barth, A.J. Strigari, L. E., Bentz, M. C., Greene, J. E., & Ho, L. C. 2009, ApJ, 690, 1031
 Bell, E.F., McIntosh, D. H., Katz, N., Weinberg, M. D. 2003, ApJS, 149, 289
 Böker, T. et al. 1999, ApJS, 124, 95
 Böker, T., Laine, S., van der Marel, R. P., Sarzi, M., Rix, H-W., & Ho, Luis C.; Shields, J. C. 2002, AJ, 123, 1389
 Bruzual, G. & Charlot S. 2009, in preparation
 Chabrier, G. 2003, ApJ, 586, 133
 Cleary, K., Lawrence, C., Marshall, J., Hao, L., & Meier, D. 2007, ApJ, 660, 117
 Dale, D.A. & The SINGs Team 2006, ApJ, 646, 161
 Dale, D.A. et al. 2009, ApJ, 693, 1821
 Deo, R.P. Crenshaw, D. M., Kraemer, S. B., Dietrich, M., Elitzur, M., Teplitz, H., & Turner, T. J. 2007, ApJ, 671, 124
 Desroches, L.-B., & Ho, L.C. 2009, ApJ, 690, 267
 Dewangan, G.C., Mathur, S., Griffiths, R. E., & Rao, A. R. 2008, ApJ, 689, 726
 Dong, X.Y. & De Robertis, M.M. 2006, AJ, 131, 1236
 Drory, N. & Fisher, D.B. 2007, ApJ, 664, 640
 Dudik, R. P., Satyapal, S., Gliozzi, M, Sambruna, R. 2005, ApJ, 620, 113
 Dudik, R. P., Weingartner, J. C., Satyapal, S., Fischer, J., Dudley, C. C., O'Halloran, B. 2007, ApJ, 664, 71
 Fabbiano, G., Kim, D.W., & Trinchieri, G. 1992, ApJS, 80, 531
 Ferrarese, L. & Merritt, D., 2000, ApJ, 539, 9
 Filippenko, A.V. & Ho, L.C. 2003, ApJ, 588, 13
 Gebhardt, K. et al. 2000, ApJ, 539, 13
 Gebhardt, K. et al. 2001, AJ, 122, 2469
 Genzel, R., Drapatz, S., Lutz, D., Wright, C., & de Graauw, Th. 1996, IAUS, 178, 373
 Ghosh, H., Mathur, S., Fiore, F., & Ferrarese, L. 2008, ApJ, 687, 216
 Giveon, U., Sternberg, A., Lutz, D., Feuchtgruber, H., Pauldrach, A. W. A. 2002, ApJ, 566, 880
 Gliozzi, Satyapal, S., Eracleous, M., Titarchuk, L.; & Cheung, C. C. 2009, ApJ, in press
 Gorjian, V., Cleary, K., Werner, M. W., & Lawrence, C. R. 2007, ApJ, 655, 73
 Goulding, A. & Alexander, D. 2009, MNRAS, in press
 Haas, M., Siebenmorgen, R., Schulz, B., Krugel, E., & Chini, R. 2005, A&A, 442, L39
 Heckman, T.M. 1980, A&A, 87, 152
 Higdon, S.J.U. et al. 2004, PASP, 116, 975
 Ho, L. C., Filippenko, A.V., & Sargent, W.L.W. 1997, ApJS, 112, 315
 Ho, L. C. et al. 2008, ApJ, 549, L51
 Houck, J. R. et al. 2004, ApJS, 154, 18
 Kauffmann, G. et al., 2003, MNRAS, 346, 1055
 Kennicutt, R.C. et al. 1998, ApJ, 498, 541
 Kewley, L.J., Dopita, M.A., Sutherland, R.S., Heisler, C.A., & Trevena, J. 2001, ApJ, 556, 121
 Knapen, J.H. et al. 2003, MNRAS, 344, 527
 Kormendy, J., & Kennicutt, R.C., 2004, ARA&A, 42, 603
 Laurikainen, E., Salo, H., Buta, R., & Vasylyev, S. 2004, MNRAS, 355, 1251
 Lira, P., Lawrence, A., O'Brien, P., Johnson, R. A., Terlevich, R., & Bannister, N. 1999, MNRAS, 305, 109
 Maloney, P.R., Hollenbach, D. J., & Tielens, A. G. G. M. 1996, ApJ, 466, 561
 Melendez, M., Kraemer, S. B., Schmitt, H. R., Crenshaw, D. M., Deo, R. P., Mushotzky, R. F., & Bruhweiler, F. C. 2008, ApJ, 689, 95
 Mendoza, C., Zeppen, C.J. 1982 MNRAS, 199, 1025
 Moran, E.C. et al. 1999, PASP, 111, 801
 Niklas, S., Klein, U., Braine, J., & Wielebinski, R. 1995a, A&AS, 114, 21
 Niklas, S., Klein, U., & Wielebinski, R. 1995b, A&A, 293, 56
 Ogle, P., Whyson, D., & Antonucci, R. 2006, ApJ, 647, 161
 Peterson, B.M. et al. 2005, ApJ, 632, 799
 Satyapal, S., Sambruna, R. M., & Dudik, R. 2004, A&A, 414, 825

- Satyapal, S., Vega, D., Heckman, T., O'Halloran, B., Dudik, R. 2007, ApJ, 663, 9
- Satyapal, S., Vega, D., Dudik, R. P., Abel, N. P., & Heckman, T. 2008, ApJ, 677, 926
- Scarlata, C. et al. 2004, ApJ, 128, 1124
- Seth, A., Agueros, M., Lee, D., & Basu-Zych, A. 2008, ApJ, 678, 116
- Shields, J.C. Walcher, C. J., Böker, T., ; Ho, L. C., Rix, H., & van der Marel, R. P.2008, ApJ, 682, 104
- Sturm, E. et al. 2002, A&A, 393, 821
- Tayal, S.S. & Gupta, G.P. 1999, ApJ, 526, 544
- Tommasin, S., Spinoglio, L., Malkan, M. A., Smith, H., González-Alfonso, E., & Charmandaris, V. 2008, ApJ, 676, 836
- Tully, R.B. & Shaya, E.J. 1984, ApJ, 281, 31
- Veilleux, S., Cecil, G. & Bland-Hawthorn, J. 2005, ARA&A, 43, 769
- Veilleux, S. & Osterbrock, D.E. 1987, ApJS, 63, 295
- Verma, A. , Lutz, D., Sturm, E., Sternberg, A., Genzel, R., & Vacca, W. 2003, A&A, 403, 829
- Vollmer, B., Thierbach, M., & Wielebinski, R. 2004, A&A, 418, 1
- Walcher, C.J., van der Marel, R. P., McLaughlin, D., Rix, H.-W., Böker, T., Hring, N., Ho, L. C., Sarzi, M., & Shields, J. C. 2005, ApJ, 618, 237
- Weedman, D. W., Hao, Lei, Higdon, S. J. U., Devost, D., Wu, Yanling, Charmandaris, V., Brandl, B., Bass, E., & Houck, J. R. 2005, ApJ, 633, 706